Online ISSN 1848-3380, Print ISSN 0005-1144
ATKAFF 55(2), 170–181(2014)

Iva Bačić, Krešimir Malarić, Milica Pejanović-Djurišić

Simulation Model for Evaluation of the DVB-SH-A Performance

DOI 10.7305/automatika.2014.01.504
UDK 621.397.4:621.371.36; 004.942
IFAC 2.3; 2.8; 5.8

Original scientific paper

This paper presents our simulation model for DVB-SH system following the ETSI standard EN 302 583. Simulation model includes DVB-SH transmitter and receiver, supports different system parameters and transmission channels. The model provides overall evaluation of DVB-SH system parameters and can be used for educational purposes.

Key words: Channel models: AWGN channel, Rayleigh, Ricean and Typical urban fading channel models, DVB-SH system, SH-A with OFDM based transmission, Simulation model

Simulacijski model za analizu parametara DVB-SH-A sustava. U radu je predstavljen naš simulacijski model za DVB-SH sustav modeliran prema ETSI normi EN 302 583. Simulacijski model uključuje DVB-SH odašiljač i prijamnik, podržava različite parametre sustava i različite prijenosne kanale. Model daje sveukupnu ocjenu komunikacije putem DVB-SH sustava i može se koristiti u edukacijske svrhe.

Ključne riječi: modeli kanala: AWGN kanal, Rayleighev, Riceov i Typical urban model kanala, DVB-SH sustav, SH-A temeljen na OFDMu, simulacijski model

1 INTRODUCTION

Today, mobile phone or other handheld device owners expect also receiving and watching a TV stream besides the classical voice or text services. The Digital Video Broadcasting – Satellite services to Handheld (DVB-SH) is designed to transport mobile TV services. It also supports a wide range of mobile multimedia services, e.g. audio and data broadcast as well as file download services [1], [2].

The DVB-SH system relies on a hybrid satellite and terrestrial infrastructure operating at frequencies below 3 GHz [3]. The DVB-SH system coverage is obtained by combining a Satellite Component (SC) and a Complementary Ground Component (CGC) [4]. The Satellite Component covers wide areas while CGC provides cellular-type coverage as well as insurance of service continuity in areas where satellite is not able to provide expected quality of service (QoS).

The system includes two different physical layer configurations:

1. SH-A based on the orthogonal frequency division multiplexing (OFDM) derived from the DVB-T standard [5]. Both, the SC and the CGC use the OFDM transmission.
2. SH-B based on time division multiplexing (TDM) transmission mode for the SC and OFDM transmission mode for the CGC. The TDM mode is partly derived from the DVB-S2 (satellite 2$^{\text{nd}}$ Generation) standard [6], [7].

The OFDM waveform is known to exhibit a larger peak-to-average signal envelope fluctuation compared to the TDM waveform. Therefore, SH-A is in general recommended for spectrum limited systems while SH-B is of interest in power limited satellite systems. However, the final choice depends on the detailed architecture of the payload.

In this paper we present the OFDM based DVB-SH simulation model, developed in Matlab. The paper is organized as follows. The DVB-SH transmitter based on the OFDM transmission at SC and CGC as well as the DVB-SH receiver are presented in Section 2. Section 3 presents simulation model and simulation results. Section 4 concludes paper.

2 THE DVB-SH-A SYSTEM CONFIGURATION

The DVB-SH performs adaptation and transmission of one or two (in hierarchical mode) baseband signals to both satellite and terrestrial channel characteristics. Baseband signals at system input are, by default, MPEG Transport Streams (MPEG TS) [8] and are composed of burst,

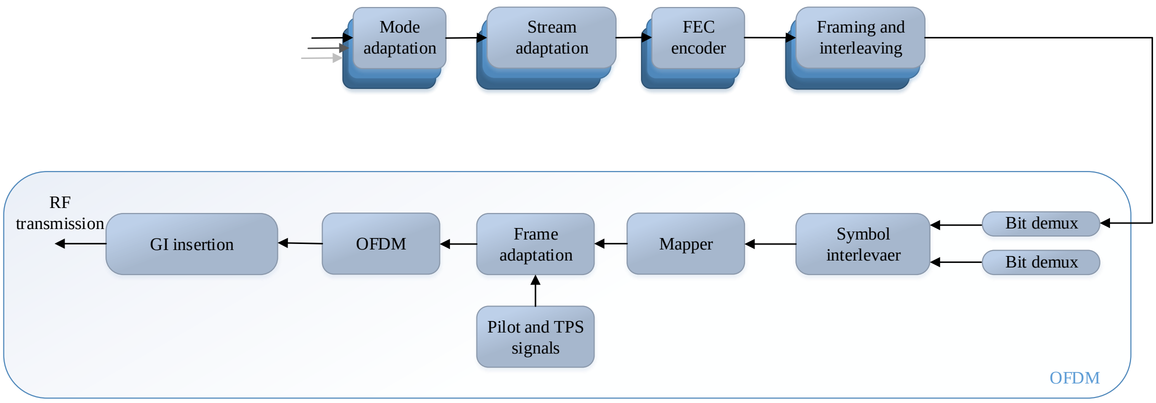

Fig. 1. DVB-SH-A transmission block diagram [1].

compliant with time slicing, defined and used in DVB-H (Handheld) [9]. Typically, a burst transports a given service, e.g. TV channel. The size of each burst may vary with time in order to support Variable burst Bit Rate [1].

The Fig. 1 describes the transmission system with OFDM for satellite path. The SH-A transmitter consists of several signal processing blocks:

- Mode adaptation: CRC-16 and insertion of Encapsulation Frame Header
- Stream adaptation: padding and scrambling of Encapsulation Frame
- Forward Error Correction, FEC code based on 3GPP2 turbo code with bit-wise interleaving,
- Framing and Convolutional time interleaving,
- Symbol interleaver,
- Bit mapping to constellation,
- OFDM framing (+ pilot and Transmission Parameter Signaling, TPS carriers),
- OFDM Transmitter and
- Guard Interval, GI insertion.

2.1 Source coding and MPEG Transport Streams

MPEG-2 transport stream is primarily intended for the transport of TV programs over long distances via transmission supports or in environments susceptible to the introduction of relatively high bit error rates (BER), higher than $1 \cdot 10^{-5}$. There also exist MPEG-2 program stream [8] (MPEG-2 PS), which is primarily intended for applications where the transmission channel or storage medium is supposed to introduce only a very low number of errors (BER $< 10^{-10}$) [1].

In our simulation model, the message is generated via a random bit generator.

2.2 Mode Adaptation

The mode adaptation takes every MPEG packet [8] and provides error detection via the CRC-16 encoder. The CRC-16 encoder provides error detection capability to upper layers. The input stream is a sequence of User Packets of length UPL (length UPL = 188 bytes), starting with a Sync-Byte. The useful part of the UP (excluding the Sync-Byte) is processed by a systematic 16-bit CRC encoder [1]. The generator polynomial is 0×1021: $g(x) = x^{16} + x^{12} + x^5 + 1$ [4].

Transportation via the DVB-SH allows other input stream modes than MPEG transport stream [8].

The Signaling process, a part of the Mode Adaptation, ensures handling of any input stream formats, packetized or not.

2.3 Stream Adaptation

The Stream Adaptation provides padding to a constant length of $\mathrm{L}_{\mathrm{TC-input}} = 12282$ bits to match the input turbo code block size. In case of MPEG-TS, 72 bits (9 bytes) of padding are required.

After padding, the stream adaptation performs scrambling. The DVB requires that energy dispersal should be undertaken before the correction process in order to obtain an evenly distributed energy within the RF channel. In order to avoid long series of 0's or 1's, which would bring DC content to the signal, the signal has to be randomized ensuring energy dispersal in the channel. This is obtained by scrambling the signal by means of a pseudo-random binary sequence (PRBS) with the generator polynomial $1+X^{14}+X^{15}$ [1]. The PRBS disperses the data but not the sync words (0×47) of the TS packets. The sync word is the first byte of each TS packet. The polynomial has a length of 1503 bytes. The generator is reinitialized by loading its register with the sequence 100101010000000. Energy dispersal ensures a constant average modulator output level [10].

2.4 FEC coding

The forward error correction is based on the 3rd Generation Partnership Project 2 (3GPP2) standard [11]. The coder in DVB-SH consists of two recursive and systematic convolutional (RSC) encoders connected in parallel (Fig. 2) [4]. One RSC encoder takes the input stream and encodes it. The other encoder takes the input stream to be encoded but performs the 3GPP2 interleaving [1] before coding. The two recursive convolutional codes are called the constituent codes of the turbo code [1], the outputs of the constituent encoders are punctured and repeated to achieve the $(\mathrm{L_{TC-input}}+6)/\mathrm{CR}$ output symbols where CR is the code rate.

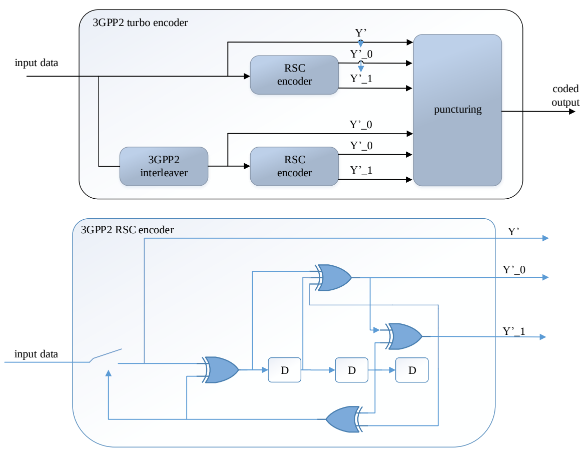

Fig. 2. Trubo encoder [1].

The turbo encoder generates an output symbol sequence that is identical to the one generated by the encoder shown in Fig. 2. Initially, the states of the constituent encoder registers in Fig. 2 are set to zero. The constituent encoder outputs are in sequence X, Y_0, Y_1, X', Y'_0, Y'_1 with the X output first to be led to the puncturing block. Puncturing patterns are defined for every used code rate; for some code rates in two different variants: the standard and complementary pattern, e.g. for code rate $= 1/2$ the standard puncturing pattern is $1;1;0;0;0;0;\ 1;0;0;1;0;$ and the complementary pattern is $1;0;0;0;1;0;\ 1;1;0;0;0;0$ (puncturing code is read from left to right). Other puncturing patterns are defined in Table 1. Within a puncturing pattern, a '0' deletes the symbol and '1' passes the symbol. The coded output data is led to OFDM mode configuration.

Table 1. Puncturing patterns for the data periods [1].

Code rate	Pattern name	Puncturing Pattern
1/5	Standard	1; 1; 1; 0; 1
2/9	Standard	1;0;1;0;1;1; 1;1;1;0;1;1; 1;1;1;0;0;1; 1;1;1;0;1;1;
1/4	Standard	1;1; 1;0;0;1 1;1;0;0;1;1;
2/7	Standard	1;0;1;0;0;1; 1;0;1;0;1;1; 1;0;1;0;0;1 1;1;1;0;0;1;
1/3	Standard	1;1;0;0;1;0;
1/3	Complementary	1;0;1;0;0;1;
2/5	Standard	1;0;0;0;0;0; 1;0;1;0;0;1; 0;0;1;0;0;1; 1;0;1;0;0;1; 1;0;1;0;0;1; 0;0;1;0;0;1; 1;0;1;0;0;1; 1;0;1;0;0;1; 0;0;1;0;0;1; 1;0;1;0;0;1; 1;0;1;0;0;1; 0;0;1;0;0;1;
2/5	Complementary	1;1;0;0;1;0; 0;1;0;0;1;0; 1;1;0;0;1;0; 1;1;0;0;1;0; 0;1;0;0;1;0; 1;1;0;0;1;0; 1;1;0;0;1;0; 0;1;0;0;1;0; 1;1;0;0;1;0; 1;1;0;0;1;0; 0;1;0;0;1;0; 1;1;0;0;1;0;
1/2	Standard	1;1;0;0;0;0; 1;0; 0;0;1;0;
1/2	Complementary	1;0;0;0;1;0; 1;1;0;0;0;0;
2/3	Standard	1;0;0;0;0;0; 1;0;0;0;0;0; 1;0;0;0;0;0; 1;0;1;0;0;1;
2/3	Complementary	1;0;0;0;0;0; 1;0;1;0;0;1; 1;0;0;0;0;0; 1;0;0;0;0;0;

2.5 Fraiming and Interleaver

In DVB-SH transmitter, the coded data is led to the framing and interleaving block.

The interleaver ensures waveform resistance to short-term fading and medium-term shadowing. First, encoded data is lead to a block bit-wise interleaver working on individual coded words. Values for block interleaving for turbo input block size of 12282 bits (payload) are given in [1]. Values for interleaving in case of signaling field may be found in [1]. The interleaved output vector is:

$$\begin{aligned} &B = (b_0, b_1, b_2, ..., b_{NTCB-1}); \\ &B_w = a_{H(w)}, \qquad w \in (0, N_{TCB-1}) \ . \end{aligned} \tag{1}$$

In (1) $a_{H(w)}$ is element of bit vector at FEC coding output, $A = (a_0, a_1, a_2, \ldots, a_{NTCB-1})$ and N_{TCB-1} is number of bits of the FEC encoded block.

2.6 Bit Demux

The SH-A standard performs demultiplexing of interleaved stream into two or four paths. In case of QPSK modulation, the stream is demultiplexed in $v = 2$ sub-streams and with the 16QAM modulation, the stream is demultiplexed into $v = 4$ sub-streams to be processed by the symbol interleaver. The demultiplexing, in case of non-hierarchical mode is defined as mapping of the input bits, x_{di} onto the output bits $b_{e,do}$:

$$x_{di} = b\left[di(\mathbf{mod})v\right](div)(v/2)+ \\ +2\left[di(\mathbf{mod})(v/2)\right], di(div)v. \qquad (2)$$

where di is the input bit number, *e* is the demultiplexed bit stream number ($0 \leq e \leq v$), mod is the integer modulo operator and *div* is the integer division operator. The hierarchical mode is not considered in this paper, but its definition may be found in [1].

2.7 Symbol interleaver

According to the OFDM mode, the symbol interleaver maps *v* bit words onto active carriers. Number of active carriers per OFDM symbol in case of 1K OFDM mode is 756 and in case of 2K OFDM mode is 1512. When 4K-mode is used, there are 3024 active carriers and in case of 8K OFDM mode, the *v*-bit words are mapped to 6048 active carriers [10].

The permutation function used in this processing block, $H(q)$ si defined as:

$q = 0;$
for $(i = 0; i < M_{max}, i = i + 1)$
$\{\ H(q) = (i \ \mathbf{mod}\ 2) \times 2^{N_r} - 1 + \sum_{j=0}^{N_r-2} R_i(j) \times 2^j;$
if $(H(q) < N_{max})\ q = q + 1;\ \}$

where M_{max} and N_{max} are parameters defined according to FFT size and are defined in [4]. N_r presents number of bits in binary word R'_i, $N_r = \log_2 M_{max}$. Parameter R'_i takes values as given in [1] and defines R_i with bit permutations depending on OFDM-mode.

2.8 Mapper

The system uses OFDM transmission. All data carriers in one OFDM frame are modulated using QPSK or 16-QAM constellation [1], [4].

Non-hierarchical transmission uses only uniform constellations. In the mapping block, assignment of the I/Q value pair takes place as shown in Fig. 3 [4]. The distance of the clouds of I/Q value pairs from the I and Q axes is determined by parameter α, which may take values 1, 2 or 4. Parametar $\alpha = 1$ is permissible in non-hierarchical modulation.

Hierarchical modulation is possible only with 16-QAM and can use all α values and two out of four bits are allocated to each path.

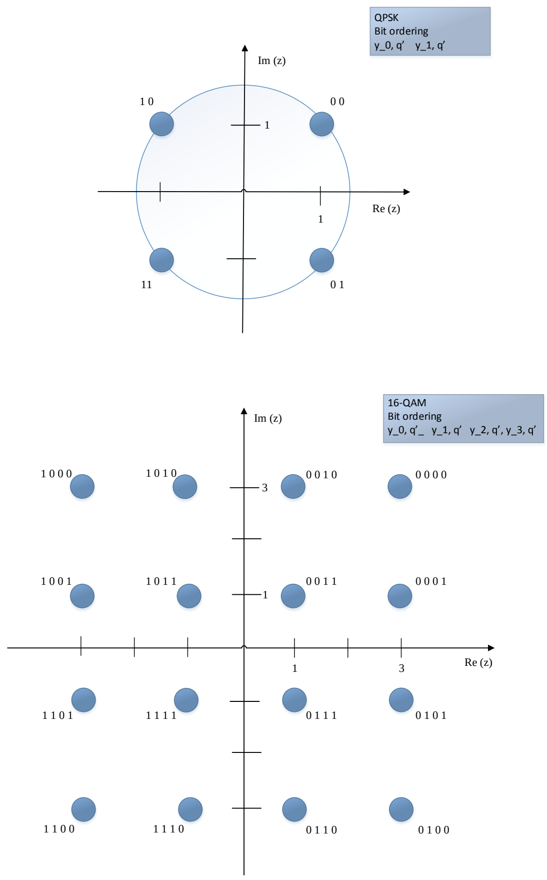

Fig. 3. QPSK and 16-QAM mapping [1].

2.9 Frame Adaptation

The frame adaptation block takes the modulated message stream and groups it into OFDM symbols. 68 consecutive symbols form one OFDM frame and 4 frames form one OFDM super-frame. The frame adaptation adds the Transmission Parameter Signals (TPS), fixed and scattered pilots as well as zero carriers on predefined locations. The pilots can be used for frame synchronization, frequency synchronization, time synchronization, channel estimation, transmission mode identification and can also be used to follow the phase noise. The carriers are indexed by $k \in [K_{min}; K_{max}]$ and determined by $K_{min} = 0$ and $K_{max} = 852$ in 1K mode, 1704 in 2K mode, 3408 in 4K mode and 6816 in 8K mode respectively [4].

Continual and scattered pilot signals, modulated with BPSK with boosted power level amplitude (by the factor 16/9), are added between useful pilots. The DVB-SH presents 177 continual pilots in the 8K mode, 89 in the 4K mode, 45 in the 2K mode and 25 in the 1K mode and they have static places in every symbol. All continual pilots are modulated according to a PRBS with the generator polynomial $X^{11} + X^2 + 1$ initialized with 11111111111 [1]. The continual pilots are transmitted at boosted power level. The use of continual pilots would be enough if communication channel would have a static characteristic. Since in real communication there is no constant channel response, the scattered pilots are used to estimate the channel in a proper way. Scattered pilots change places in every symbol, and every 4th symbol they repeat their place. For the symbol of index 1 (ranging from 0 to 67), carriers for which index k belongs to the subset $\{k = K_{min} + 3x(1\text{mod}4) + 12p \mid p\,\text{integer}, p \geq 0, k \in [Kmin; Kmax]\}$ are scattered pilots. Parameter p is an integer that takes all possible values greater than or equal to zero, provided that the resulting value for k does not exceed the valid range $[K_{min}; K_{max}]$.

TPS bits are also sent between useful carriers. TPS carriers are only modulated along the I axis and so are a direct indication of the phase. The TPS is transmitted in parallel on 7 TPS carriers in 1K mode, 17 carriers for the 2K mode, on 34 carriers for the 4K mode and on 68 carriers for the 8K mode. Every TPS carrier in the same symbol conveys the same differentially encoded information bit. The TPS are DBPSK modulated and indicate [10]:

- modulation type (including α value);
- hierarchy information;
- guard interval;
- transmission mode (1K, 2K, 4K or 8K);
- frame number in a super-frame;
- cell identification;
- DVB-SH mode (selector bit);
- Code rates;
- Time interleaver configuration and
- Super frame number in a SH frame.

2.10 OFDM Transmitter

OFDM modulation consists of N closely spaced orthogonal carriers of duration T_0 (each one is modulated with a conventional modulation scheme), with a spacing of $1/T_0$ between two consecutive carriers. Increasing the number of carriers does not modify the payload bit rate, which remains constant. The OFDM transmitter performs the transform into the time domain using Inverse Fast Fourier Transformation, (IFFT) [12].

2.11 Guard Interval insertion

Every OFDM block is extended, prefixing the end of the block to its beginning (called the Guard Interval, GI or Cyclic Prefix, CP). The cyclic prefix serves as a guard interval and eliminates the intersymbol interference from the previous symbol. Insertion of the guard interval extends symbol duration by 1/4, 1/8, 1/16 or 1/32 to give the total symbol duration T_S [4]. The time signal of length, T_S is still complex [10].

2.12 DAC and front-end

Digital signal is transformed into an analogue signal, with a digital to analog converter and then modulated to radio frequency (VHF, UHF) by the RF front-end. The occupied bandwidth is designed to accommodate DVB-SH signal into 1.7, 5, 6, 7 or 8 MHz channels. The base band sample rate provided at the DAC input depends on the channel width:

$$f_s = \frac{8}{7}B \quad [\text{MHz}] \ , \tag{3}$$

where *B* is the channel width in Hz [10].

The signal to be transmitted through channel is filtered with Root Raised Cosine filter with the roll-off factor set to 0.25 [4].

Spectrum of the signal at the receiver input is shown in Fig. 4.

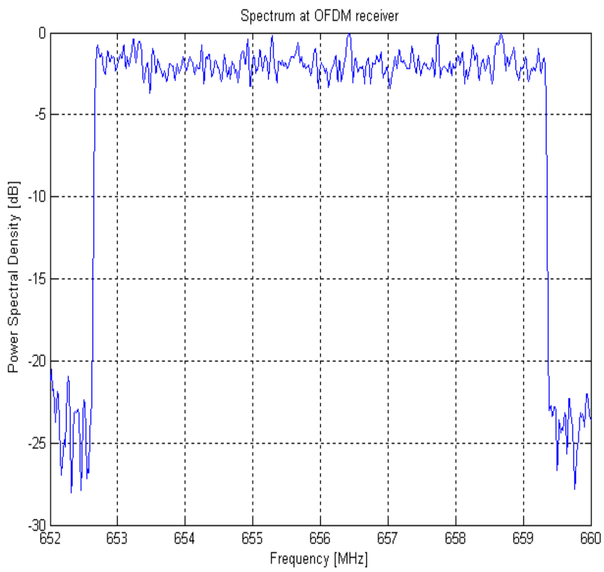

Fig. 4. Spectrum of OFDM signal (gained with simulation model).

2.13 Technical description of a DVB-SH receiver

The DVB-SH receiver consists of below described signal processing blocks:

- Front-end and ADC;
- Time and frequency synchronization;
- Guard interval disposal and OFDM Receiver;
- Channel Estimator and Channel Compensation;
- Demapper;
- Deinterleaver;
- Decoding;
- MUX adaptation;
- MPEG demultiplexing and source decoding.

The receiving set-top box adopts techniques which are dual to the ones used in the transmission. Its practical performance depends on hardware construction; it is not standardized like encoder.

An important part of the receiver is the channel estimation part. In real communication, channel frequency response is unknown. Our channel estimation is based on the Zero-forcing (ZF) method [13]. ZF inverts the frequency response of the channel. At the receiver side, input has to be multiplied with ZF:

$$ZF = \frac{H^*}{|H|^2} = \frac{1}{H} \tag{4}$$

where *H* is channel estimation based on pilot carriers [10]. To obtain the channel characteristic, interpolation has to be done. The ETSI standard defines ideal channel knowledge but in our simulation, interpolation is done since ideal channel knowledge is not possible. This results in different communication quality when compared to the quality introduced by the standard.

Another important part is the decoder. In this simulation, the turbo decoding process was done via the Soft-Input Soft-Output maximum a-posteriori algorithm [14], [15]. The DVB-SH standard allows different iteration numbers for the decoder process, but according to [1], [4] this number should be set to 8. In all our simulations, the iteration number was set to 8.

3 SIMULATION MODEL AND RESULTS

The transmitter and receiver, introduced in Section 2 are adopted to form a simulation model of the DVB-SH system. Already, a DVB-SH simulation model based on OFDM transmission is presented in [16]. But mentioned simulation model did not cover the FEC scheme described in Section 2 and adopted by [1]. Unlike the model in [16], in this paper we present a simulation model of the DVB-SH based on OFDM that adopts the 3GGP2 turbo encoder as well. The simulation model is designed via Matlab.

Prior to simulation, different parameters can be chosen and defined:

- Modulation type ($\alpha = 1$): QPSK or 16-QAM;
- FEC: 1/5, 2/9, 1/4, 2/7, 1/3, 2/5, 1/2, 2/3;
- OFDM mode: 1K, 2K, 4K or 8K;
- guard interval: 1/4, 1/8, 1/16, 1/32;
- Speed of receiver;
- Carrier frequency: 656 MHz;
- SNR, noise level in channel.

After choosing system parameters the simulation may be done. Simulation results are constellation diagram (see Fig. 5 gained with simulation model) and spectrum of the signal at the input of receiver (result of simulation given in Fig. 4). Additionally, bandlimited impulse response of fading channels can also be shown, but it slows simulation down. Finally, BER is calculated.

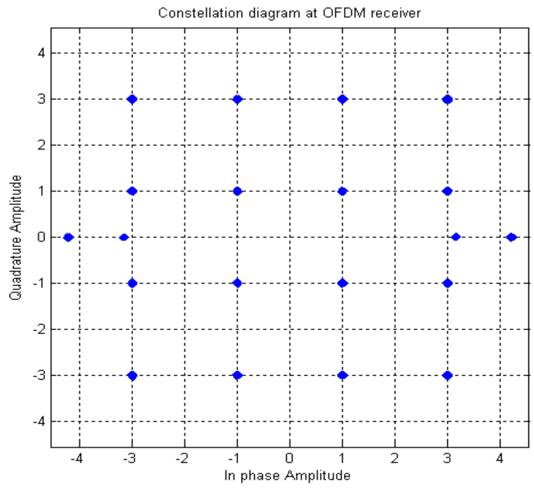

Fig. 5. Constellation diagram for the 16-QAM at C/N=20 dB.

The simulation will be tested over different channel models. The most suitable models for DVB-SH satellite channels are statistical models. The statistical land mobile satellite (LMS) propagation model is characterized by parameters that have been derived through synthetic time series matching with experimental data obtained in different LMS propagation environments [1], [4]. Statistical models for satellite channels assume that the received signal is composed of two parts - a coherent part associated with the Line of Sight (LOS) path and a diffuse part arising from multipath components.

In this paper, simulation results are obtained by observing transmission over fixed terrestrial channel models. The Gaussian and Rayleigh channel models, already designed for the DVB-H [17], [18] could be used for simulation in DVB-SH as well.

Besides the mentioned fading channels, another mobile channel model reproduces the terrestrial propagation in an urban area. The typical urban (TU6) profile is defined by COST 207 [19] and is made of 6 paths having wide dispersion in delay and relatively strong power. But at low speeds (i.e. pedestrian situations), new channel models have been developed by the Wing-TV project [20]–[21]. These are the Pedestrian Indoor (PI) and the Pedestrian Outdoor (PO) channel models. These new models were created especially for describing the slowly moving handheld reception indoors and outdoors [20].

In following section the required C/N in dB for error-free reception (where BER is equal to $1 \cdot 10^{-5}$) is calculated over three different channel models: the Gaussian AWGN, the Ricean and the Rayleigh fading channel models.

3.1 Gaussian channel

In our first experiment, we used Gaussian channel with added white noise only.

Different combinations of modulation and FEC schemes are tested. In all experiments the 1K OFDM mode was used with a guard interval fixed to 1/4. The signal to noise ratio was adjusted so that the bit error rate does not exceed the $1 \cdot 10^{-5}$. Our simulation results are compared to the C/N rate for error-free communication introduced in the ETSI standard. Our application uses real channel estimation, while ETSI standard uses "perfect channel estimation". The perfect channel estimation presumes that fading impact was known at the receiver side so it is multiplied with its inverted characteristic.

Results are shown in Table 2 where the influence of channel estimation in case of AWGN channel is listed, too. The influence of channel estimation in case of communication over a common Gaussian AWGN channel is also given in Fig. 6 showing the constellation graph for the QPSK modulated and FEC 2/3 protected communication over an AWGN channel. In first case the receiver performs estimation of channel, while in second case no estimation is made. Constellation graphs for these two studies are presented. Constellation graphs are gained as simulation results. Table 2 shows that our results are similar to the results provided by the ETSI standard. Difference in C/N levels for error-free communication is the result of channel estimation. The ETSI standard introduces perfect channel

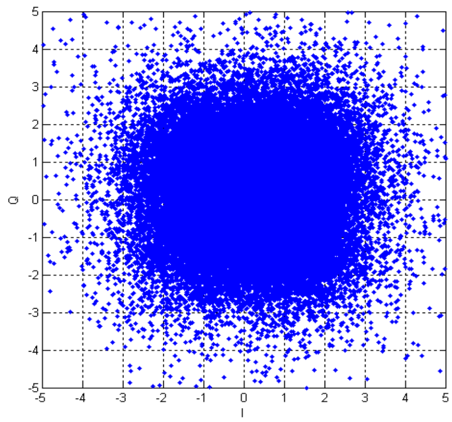

(a) With channel estimation

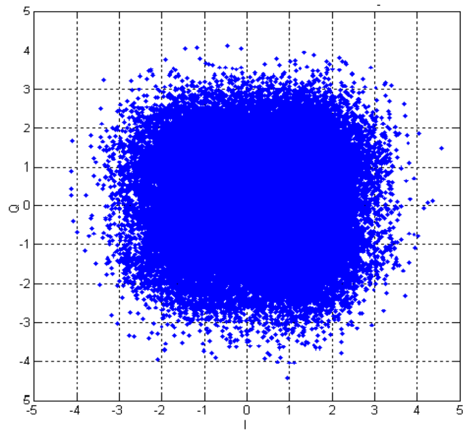

(b) Without channel estimation

Fig. 6. Constellation diagram for QPSK 2/3 communication over AWGN (C/N = -2 dB).

Table 2. Required C/N (dB), Gaussian channel.

QPSK code rate	ETSI standard, C/N (dB)	Our results, C/N (dB) with channel estimation	Our results, C/N (dB) no channel estimation
1/5	-3.6	-3	-3.8
1/4	-2.5	-2	-3.5
2/7	-1.8	-1.3	-3
1/3	-0.9	-1.1	-2.8
2/5	0.1	-1	-2.2
1/2	1.4	1.5	-0.3
2/3	3.5	5	0.2
16QAM code rate	**ETSI standard, C/N (dB)**	**Our results, C/N (dB) with channel estimation**	**Our results, C/N (dB) no channel estimation**
1/5	0.7	0.7	1.1
1/4	1.9	2.0	1.8
2/7	2.8	3.5	2.8
1/3	3.7	3.7	2.9
2/5	5.0	3.8	3
1/2	6.8	6.3	6
2/3	9.7	8.2	7.5

estimation (perfect channel knowledge). To obtain channel characteristics, linear interpolation was done. Interpolation introduces certain deviation from C/N valued for QEF listed in ETSI standard that may be seen in Table 2. The level of noise for a proper error-free communication with channel estimation at receiver was compared to the noise level when no channel estimation was used. Results in Table 2 show that the channel estimation introduces errors as a result of the mentioned linear interpolation. The error is perceived in lower level of noise allowed in channel for error free communication. Both, the QPSK and the 16-QAM modulation were examined. Results show that the QPSK is more robust then the 16-QAM modulation scheme but in this case, useful data rate is lower since there are only two bits per symbol.

3.2 Ricean fading channel

In the second experiment, Ricean fading has been introduced. The Ricean channel is a transmission channel that may have one line-of-sight (direct) component that has usually higher power and several scattered, phase shifted and time delayed, multipath components. Ricean channel is used for fixed reception and is described as [10]:

$$y(t) = \frac{\rho_0 \cdot x(t) + \sum_{i=1}^{N} \rho_i \cdot e^{-j \cdot \theta_i} \cdot x(t-\tau_i)}{\sqrt{\sum_{i=0}^{N} \rho_i^2}}, \quad (5)$$

where N is number of echoes, θ_i is the phase shift from scattering of the i-th path, ρ_i is the attenuation of the i-th path, τ_i is the relative delay of the i-th path. Case $i = 0$ describes direct path. Ricean factor K (ratio of the power of the direct path to the reflected paths) is given as [10]:

$$K = \frac{\rho_0^2}{\sum_{i=1}^{N} \rho_i^2}. \quad (6)$$

In our simulation we used K=10 dB. Parameters of the simulated paths are given in Table 3 [10].

The DVB-SH system was tested while communication was established via different combinations of modulation and FEC schemes over a Ricean fading channel. Again, like in case of Gaussian channel, the needed C/N rate for quasi error-free communication was claimed and listed in Table 4 (receiver performs channel estimation in all observed cases of communication).

It may be seen that a higher code rate requires a higher C/N for QEF communication. In case of a low code rate, e.g. 1/5 the protection over 1 message bit is gained via 4 parity bits while in case of a higher code rate like the

Table 3. Normalized amplitude (overall power 0dB), phase and delay values for simulated Ricean and Rayleigh channel.

i	$\rho_{i\,(Ricean)}$	$\rho_{i\,(Rayleigh)}$	Delay(μs)	θ_i (rad)
0	0.953462	-	0	0
1	0.016187	0.053687	1.003019	4.855121
2	0.049635	0.164620	5.422091	3.419109
3	0.114301	0.379093	0.518650	5.864470
4	0.085224	0.282656	2.751772	2.215894
5	0.072647	0.240941	0.602895	3.758058
6	0.017358	0.057568	1.016585	5.430202
7	0.042204	0.139975	0.143556	3.952093
8	0.014467	0.047981	0.153832	1.093586
9	0.051955	0.172315	3.324866	5.775198
10	0.112561	0.373324	1.935570	0.154459
11	0.083017	0.275336	0.429948	5.928383
12	0.098485	0.326639	3.228872	3.053023
13	0.073805	0.244784	0.848831	0.628578
14	0.063414	0.210321	0.073883	2.128544
15	0.048003	0.159207	0.203952	1.099463
16	0.042031	0.139401	0.194207	3.462951
17	0.067413	0.223585	0.924450	3.664773
18	0.032729	0.108549	1.381320	2.833799
19	0.062084	0.205908	0.640512	3.334290
20	0.072913	0.241824	1.368671	0.393889

1/2 one message bit is protected only with one parity bit. Therefore, lower code rates allow higher noise level in system (for same communication quality), the code rate itself provides already a good protection in case of errors in communication.

3.3 Rayleigh fading channel

In the third experiment, Rayleigh fading has been introduced. Its path parameters are defined in Table 3 [5]. It can be seen that this fading has no direct path (first row in Table 3) like Ricean fading introduced in Subsection 3.2 meaning that this model is useful in heavily build-up cities with many buildings.

The two modulation types used by the SH-A, the QPSK and the 16-QAM, were combined with different coding rates and the required C/N rate for quasi error-free communication was calculated via our simulation model. In all experiments, the OFDM-mode was constant (1K) and the guard interval was fixed to 1/4.

Results gained with communication over the Rayleigh fading channel are listed in Table 5.

Unlike the Ricean fading channel, the Rayleigh fading channel has no direct path. With Rayleigh channels, high fades in frequency characteristic have major impact on quality of reception and simulation results show that only robust modulations will gain stable reception.

3.4 Typical urban, TU6 channel

In the forth simulation, transmission over the typical urban channel with 6 taps, the TU6 was analyzed. The

Table 4. Required C/N (dB), Ricean channel.

QPSK code rate	Our results, C/N (dB) Ricean fading channel
1/5	-2.4
1/4	-1.8
2/7	-1.2
1/3	-0.8
2/5	0.9
1/2	2
2/3	4.8
16QAM code rate	**Our results, C/N (dB) Ricean fading channel**
1/5	3
1/4	3.2
2/7	3.5
1/3	3.8
2/5	5.1
1/2	7.5
2/3	8.5

Table 5. Required C/N (dB), Rayleigh fading channel.

QPSK code rate	C/N (dB), Rayleigh fading channel
1/5	1
1/4	1.8
2/7	2.3
1/3	2.5
2/5	3
1/2	5.5
2/3	6
16QAM code rate	**C/N (dB), Rayleigh fading channel**
1/5	6
1/4	7.2
2/7	7.5
1/3	7.6
2/5	9
1/2	11.1
2/3	12

TU6 is used for terrestrial mobile networks and is composed of tapped delay line (TDL) with 6 taps [19]. Each tap is defined with its delay and an average attenuation power (Table 6) on top of which a unit power Rayleigh complex fading process is applied. The Rayleigh fading is characterized by a Jakes Doppler Power Spectral Density profile [22]:

$$S(f) = \frac{1}{\pi f_D \sqrt{1-(f/f_D)^2}} rect(\frac{f}{2f_D}), \tag{7}$$

where f_D is the maximum Doppler frequency defined as:

$$f_D = v \cdot (\frac{f_0}{c}). \tag{8}$$

In (8) f_0 is the carrier frequency, c is the speed of light ($c = 3 \cdot 10^8$ m/s) and v is the speed of receiver.

Table 6. Typical urban channel, TU6 with Rayleigh fading distribution and Jakes Doppler spectrum.

Tap number	Delay (μs)	Average power (dB)
1	0.0	-3.0
2	0.2	0.0
3	0.5	-2.0
4	1.6	-6.0
5	2.3	-8.0
6	5.0	-10.0

Simulation results are gained for the 2K OFDM transmission with QPSK or the 16-QAM modulation with different coding rates. System parameters have been chosen with respect to mobile channel model parameters. For the minimization of negative effect of Doppler shift, modulation QPSK and 2K OFDM mode were used. Guard interval was set to $1/16$ since the maximum relative delay of the signal echo in TU6 is equal to $5\,\mu$s [15], [23]. Speed of receiver was set to $v = 50\,$km/h (maximum speed in urban areas in Croatia). The results are given in Table 7.

Table 7. Required C/N (dB), Typical urban channel.

QPSK code rate	Our results, C/N (dB) with channel estimation
1/5	-0.5
1/4	0.2
2/7	2.0
1/3	2.2
2/5	2.3
1/2	4
2/3	6.8
16QAM code rate	**Our results, C/N (dB) with channel estimation**
1/5	3.7
1/4	5.0
2/7	6.3
1/3	6.3
2/5	6.4
1/2	7.6
2/3	7.8

The communication quality for different C/N ratios and over different channel models is shown in Fig. 7. The QPSK modulation was used and the code rate was fixed to 1/5. The multiplex parameters were set to 2K OFDM with a guard interval of 1/16. In case of the typical urban channel, the receiver speed was defined as maximum allowed speed in urban areas in Croatia. In all simulated cases, the bit error rate curve has the shape of a waterfall, meaning that for lower C/N values the BER is higher. When increasing the signal-to-noise ratio, the BER is lower meaning that communication quality gets better and with fewer errors. Figure 7 shows that communication over the Rayleigh fading channel model requires the higher C/N ratio for same BER (e.g. the BER for QEF communication) when compared to other BER curves in Fig. 7.

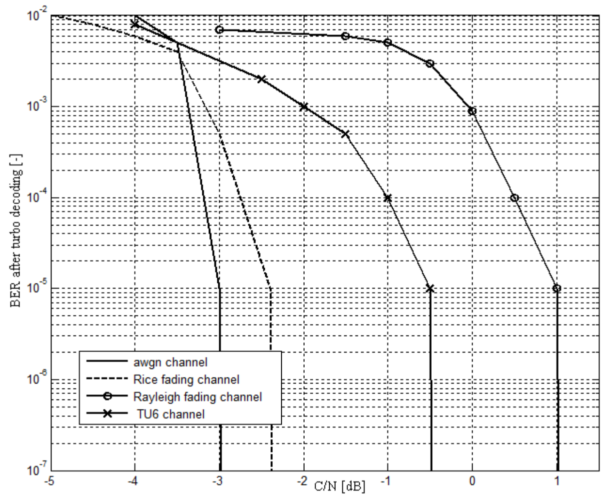

Fig. 7. Bit Error Rate for communication over the different channel models with system parameters: QPSK1/5, 2K OFDM, $\mathrm{GI} = 1/16$ *and for TU6* $v = 50$ *km/h.*

Lowest C/N for same BER is required when communication is established over the AWGN channel. In between, there are the communication over the Rice fading channel and communication established over the TU6 channel.

3.5 Guard interval influence in DVB-SH

Finally, the influence of the guard interval was explored. The guard interval is a part of the symbol that extends the message, like prefixing of a symbol with repetition of the symbol's end. This method retains the continuity of symbol.

The DVB-SH standard introduces four different guard interval durations: 1/4, 1/8, 1/16 and 1/32 of symbol length. The influence of guard interval length is analyzed for three different communication channels (introduced in Subsections 3.1 – 3.3). The used modulation was the QPSK with FEC coding 1/5. OFDM mode was chosen to be 1K. The required C/Ns in dB for quasi error communication are listed in Table 8. In case of AWGN channel the guard interval has no influence. The Gaussian channel is no multipath channel and the guard interval influence is visible only in multipath channels, like the Ricean and Rayleigh fading channels. Results show that the use of guard interval has influence on communication quality on fading channels. Our results show that a longer guard interval (e.g. guard interval of length=1/4) requires a lower C/N for error free communication as a result of greater communication protection.

4 CONCLUSION

In this paper we presented our simulation model for the digital video broadcasting – satellite to handhelds communication system.

Table 8. Required C/N (dB) for QEF communication, guard interval influence.

QPSK 1/5, 1K OFDM	AWGN channel	Ricean fading channel	Rayleigh fading channel
GI=1/4	-3	-2.4	1
GI=1/8	-3	-2.3	1.2
GI=1/16	-3	-2.2	1.2
GI=1/32	-3	-1.9	1.4

First, the DVB-SH transmitter and receiver that the model is based on were presented. The system was tested by simulating transmission over the Gaussian AWGN channel. The noise level where error-free communication is still able was matter of query. Gained results were compared to the noise level (required for QEF communication) introduced by the ETSI standard. Results show that our model has similar performances like the model defined in the ETSI standard. Differences in noise levels are the result of channel estimation since our model uses real channel estimation while the ETSI standard defines communication with ideal channel knowledge. The differences in these two ways of channel estimation result in a different noise level needed in the system for error-free communication.

The system was tested through communication over two fading channels: the Ricean fading and the Rayleigh fading channel as well as the more appropriate channel model for handheld reception, the Typical Urban channel model. The Ricean and the Rayleigh fading channel are used for modeling communication in urban areas where multipath communication is present. The difference between the two introduced fading channel models is in the direct line. While the Ricean fading channel has one line-of-sight, direct component that has usually higher power and several multipath components, the Rayleigh fading channel has no direct path but only several scattered, phase shifted and time delayed multipath components. This results in higher C/N level for error free communication in case of Rayleigh fading channel profile (compared to the Ricean fading channel).

The Typical Urban channel model takes advantage of 6 taps with its delay and an average attenuation power on top of which a unit power Rayleigh complex fading process is applied. The communication quality established over the TU6 channel was compared to communication over other introduces channel models. Communication over the Rayleigh fading channel model required the highest C/N ratio for one chosen BER (e.g. the BER for QEF communication). Lowest signal-to-noise ratio for same BER is required when communication is established over the AWGN channel. In between, there are the communication over the Rice fading channel and communication over the typical urban channel.

The influence of the guard interval and its length was tested via simulation. In case of AWGN the guard interval shows no influence since this channel model is no multipath channel model. While in tested multipath channel models (the Ricean and the Rayleigh channel models), the results show that in case of a shorter guard interval (e.g. guard interval of length 1/16) compared to a longer (e.g. guard interval of length 1/4) requires a higher C/N for same communication quality (in simulation: error free communication).

Simulation results show that our model provides an overall evaluation of DVB-SH system parameters. Next step is to design other channel models, shown to be more suitable for modeling communication in urban areas with slowly moving receivers: the pedestrian indoor and outdoor models.

ACKNOWLEDGMENT

The work described in this paper was financially supported by the Ministry of Science, Education and Sports of the Republic of Croatia (under grant number 036-0361566-1569) and by the Mediterranean Office for Youth, Paris, France.

REFERENCES

[1] TS 102 584 V1.3.1. Digital Video Broadcasting (DVB); Guidelines for Implementation for Satellite Services to Handheld devices (DVB-SH) below 3GHz, Technical Specification ETSI, 2011.

[2] TS 102 831 V1.2.1. Digital Video Broadcasting (DVB); Implementation guidelines for a second generation digital terrestrial television broadcasting system (DVB-T2), Technical Specification ETSI, 2012.

[3] M. Cohen, C. leFloch, J.M. Hanriot, S. Wilkus, G. Pousset, DVB-SH field trials Measurements Results, In Proceedings of the International Workshop on Signal Processing for Space Communication, pp530-537, Italy, 2010

[4] EN 302 583 V1.2.1. Digital Video Broadcasting (DVB); Framing Structure, channel coding and modulation for Satellite services to Handheld devices (DVB-SH) below 3GHz, European Standard ETSI, 2011.

[5] ETSI EN 300 744 V1.6.1, Digital Video Broadcasting (DVB); Framing structure, channel coding and modulation for Digital Terrestrial television, European Standard ETSI, 2009.

[6] ESTI EN 302 307 V1.2.1, Digital Video Broadcasting (DVB); Second generation framing structure, channel coding and modulation systems for Broadcasting, Interactive Services, News Gathering and other broadband satellite applications (DVB-S2), European Standard ETSI, 2009.

[7] L. Polak; T. Kratochvil, Analysis and Simulation of the Transmission Distortions of the Mobile Digital Television DVB-SH Part 2: Satellite mode DVB-SH-B with TDM. Radioengineering, 2012, vol. 21, no. 1, pp. 126-133

[8] ETSI TS 101 154 V.1.11.1, Digital Video Broadcasting (DVB); Specification for the use of Video and Audio Coding in Broadcasting Applications based on the MPEG-2 Transport Stream, July 2012

[9] ETSI EN 302 304 V1.1.1, Digital Video Broadcasting (DVB); Transmission System for Handheld Terminals (DVB-H), European Standard ETSI, 2004.

[10] E. Dumic, G. Sisul, S. Grgic, "Evaluation of Transmission Channel Models Based on Simulations and Measurements in Real Channels" Frequenz. Volume 66, Issue 1-2, ISSN (Online) 2191-6349, ISSN (Print) 0016-1136, DOI: 10.1515/freq.2012.prelims1, February 2012

[11] 3GPP2 c.S0002-D V.2.0 (2004-10). 3GPP2, Physical Layer Standard for cdma2000 Spread Spectrum Systems, 3rd Generation Partnership Project 2, 2004.

[12] R. van Nee, R. Prasad, OFDM for wireless multimedia communications, Artech House 2000.

[13] K. Fazel, S. Kaiser, "Multi-Carrier and Spread Spectrum Systems", Second Edition, Wiley, 2008

[14] S. Benedetto, G. Monotorsi, D. Divsalar, F. Pollara, "A soft-input soft-output maximum a posteriori (MAP) module to decode parallel and serial concatenated codes", The Telecommunications and Data Acquisition Progress Report, TDA PD 42-127, July-September 1996, pp 1-20.

[15] L. Hanzo, T.Liew, B. Yeap, "Turbo Coding, Turbo Equalization and Space-Time Coding for Transmission over Fading Channels, John Wiley & Sons, LTD, 2002.

[16] L. Polak, T. Kratochvil, Analysis and simulation of the transmission distortions of the mobile digital television DVB-SH Part1: Terrestrial mode DVB-SH-A with OFDM. Radioengineering, 2011, vol. 20, no. 4, pp 952-960.

[17] L. Polak, T. Kratochvil, Simulation of DVB-H transmission in Gaussian and fading channels, In Proceedings ELMAR -2010, Zadar (Croatia): ITG, Zagreb, 2010, pp.231-234, ISBN; 987-953-7044-11-4.

[18] L. Polak, T. Kratochvil, Transmission of the DVB-H in Mobile TV Mode over Fading Channels. In Proceedings of the 33rd International Conference on Telecommunications and Signal Processing (TSP 2010). Baden near Vienna (Austria), 2010, pp. 377-381

[19] COST 207: Digital land mobile radio communications (final report), Commission of the European Communities, Directorate General Telecommunications, 1898, pp. 135-147, under the direction of M. Failly

[20] PR D4 (Laboratory Test Results), Services to wireless, integrated, nomadic, GPRS-UMTS and TC Handheld Terminals, Wing TV, 2006.

[21] SR, D15, CP2-032, Services to Wireless, Integrated, Nomadic, GPRS-UMTS and TV handheld terminals, WING TV, 2006

[22] A. Bolea Alamanac, P. Burzigotti, M. Cohen, R. Gaudenzi, G. Kiva, S. Lipp, R. Puvirenti, L. Roullet, H. Stadali, Performance Validation of the DVB-SH Standard for Satellite/Terrestrial Hybrid Mobile Broadcasting Networks, IEEE Transactions on Broadcasting, vol. 57, no. 4, pp. 802-825, 2011

[23] F. Borko, A. Syed, Handbook of Mobile Broadcasting, DVB-H, DMB, ISDB-T and MEDIAFLO (Internet and Commucniations), Auerbach Publications, 2008

Iva Bačić (1984) graduated electrical engineering at University of Zagreb, Faculty of Electrical Engineering and Computing, Zagreb, Croatia in 2008. Since May 2008, she has been working as a research assistant at the Faculty of Electrical Engineering and Computing, Zagreb. Currently she is pursuing her Ph.D in wireless communication at the same Faculty. Her research focus is on digital broadcasting of satellite services to mobile handhelds as well as propagation channels in urban areas. She published 13 scientific papers and was enrolled in the program of the Mediterranean Office for Youth, Paris in the year 2012/2013.

Krešimir Malarić was born in Zagreb, Croatia in 1969. He graduated and received his master and doctoral degrees in the field of electrical engineering at the University of Zagreb, Faculty of Electrical Engineering and Computing, Zagreb in 1991, 1994 and 2000, respectively. From January 1992 until December 1995 he is employed at the Faculty of electrical engineering, Department of Fundamentals of Electrical Engineering and Measurements in Zagreb. Since January 1996 until today he is employed at the Department of Wireless Communications, Faculty of Electrical Engineering in Zagreb. In 1992 he did a specialisation at the ORF in Vienna and a postdoctoral research at the University of Bologna, Italy in 2005. In March 2011 K. Malarić was elected Full Professor at University of Zagreb. He has participated in five research projects of the Croatian Ministry of Science, Education and Sports and in two international projects. Currently he leads the research project "Laboratory for Electromagnetic Compatibility and Biological Effects of Electromagnetic Fields" funded by the Croatian Ministry of Science, Education and Sports. He has published more than 120 papers in the field of electromagnetic compatibility, biological effects of electromagnetic fields and satellite communications in scientific journals and conference proceedings. Prof. K. Malarić is an IEEE member and a member of the Croatian Academy of Engineering (HATZ). He participated in two international scientific conference program committees, is member of two editorial boards of scientific journals and reviewer in international journals. At conferences CPEM2002 in Ottawa, Canada and at the IEEE EMC 2003 in Boston, USA, K. Malarić received the award "Young Scientist Grant" and "Disadvantaged Engineer". In 2005 he received the "Gugliemo Marconi Award" in Bologna, Italy.

Milica Pejanović-Djurišić is full professor in telecommunications at the University of Montenegro, Faculty of Electrical Engineering. She is also Director of its Centre for Telecommunications. Mrs. Pejanovic-Djurisic graduated in 1982 at the University of Montenegro with BSc degree in Electrical Engineering. She has got MSc and PhD degrees in Telecommunications at University of Belgrade in 1984 and 1987, respectively. She has published more than 200 scientific papers in international and domestic journals and conference proceedings. Her main research interests are: wireless communications theory, wireless networks performance improvement, broadband transmission techniques, optimization of electronic communication development policy. She has considerable industry and operating experiences working as industry consultant (Ericsson, Siemens) and Telecom Montenegro Chairman of the Board. She has taken part in many internationally and EU funded ICT projects with domestic and international partners. She is an evaluation expert for EU FP7 projects in the field of ICT and a member of IEEE and IEICE. Prof. Pejanovic-Djurisic has also a considerable experience in the field of electronic communication regulation. Being an ITU expert, she participates in a number of missions and ITU activities related with regulatory issues, development strategies and new technological solutions. Prof. Pejanovic-Djurisic has been elected Member of the State Presidency of Montenegro (1990-1992), Member of the Parliament of Montenegro (1993-2001), Ambassador of Serbia & Montenegro in Belgium and Luxembourg, and the first Ambassador of Montenegro in France and UNESCO (2007-2010).

AUTHORS' ADDRESSES

Iva Bačić
Prof. Krešimir Malarić, Ph.D.
Faculty of Electrical Engineering and Computing
University of Zagreb
Zagreb, Croatia
email: iva.bacic@fer.hr, kresimir.malaric@fer.hr

Prof. Milica Pejanović-Djurišić, Ph.D.
Faculty of Electrical Engineering
University of Montenegro
Podgorica, Montenegro
email: milica@ac.me

Received: 2013-03-04
Accepted: 2013-06-14